






MicroRNAs of Epstein-Barr Virus Attenuate T-Cell-Mediated Immune Control *In Vivo*

Anita Murer,^a Julia Rühl,^a Andrea Zbinden,^b Riccarda Capaul,^b  Wolfgang Hammerschmidt,^c  Obinna Chijioko,^{a,d}  Christian Münz^a

^aViral Immunobiology, Institute of Experimental Immunology, University of Zürich, Zürich, Switzerland

^bInstitute of Medical Virology, University of Zürich, Zürich, Switzerland

^cResearch Unit Gene Vectors, Helmholtz Zentrum München, German Research Center for Environmental Health and German Centre for Infection Research (DZIF), Partner Site Munich, Munich, Germany

^dInstitute of Pathology and Medical Genetics, University Hospital Basel, Basel, Switzerland

ABSTRACT The human persistent and oncogenic Epstein-Barr virus (EBV) was one of the first viruses that were described to express viral microRNAs (miRNAs). These have been proposed to modulate many host and viral functions, but their predominant role *in vivo* has remained unclear. We compared recombinant EBVs expressing or lacking miRNAs during *in vivo* infection of mice with reconstituted human immune system components and found that miRNA-deficient EBV replicates to lower viral titers with decreased frequencies of proliferating EBV-infected B cells. In response, activated cytotoxic EBV-specific T cells expand to lower frequencies than during infection with miRNA-expressing EBV. However, when we depleted CD8⁺ T cells the miRNA-deficient virus reached similar viral loads as wild-type EBV, increasing by more than 200-fold in the spleens of infected animals. Furthermore, CD8⁺ T cell depletion resulted in lymphoma formation in the majority of animals after miRNA-deficient EBV infection, while no tumors emerged when CD8⁺ T cells were present. Thus, miRNAs mainly serve the purpose of immune evasion from T cells *in vivo* and could become a therapeutic target to render EBV-associated malignancies more immunogenic.

IMPORTANCE Epstein-Barr virus (EBV) infects the majority of the human population and usually persists asymptotically within its host. Nevertheless, EBV is the causative agent for infectious mononucleosis (IM) and for lymphoproliferative disorders, including Burkitt and Hodgkin lymphomas. The immune system of the infected host is thought to prevent tumor formation in healthy virus carriers. EBV was one of the first viruses described to express miRNAs, and many host and viral targets were identified for these *in vitro*. However, their role during EBV infection *in vivo* remained unclear. This work is the first to describe that EBV miRNAs mainly increase viremia and virus-associated lymphomas through dampening antigen recognition by adaptive immune responses in mice with reconstituted immune responses. Currently, there is no prophylactic or therapeutic treatment to restrict IM or EBV-associated malignancies; thus, targeting EBV miRNAs could promote immune responses and limit EBV-associated pathologies.

KEYWORDS Epstein-Barr virus, cytotoxic T cells, humanized mice, immune escape, lymphoma, miRNA

Epstein-Barr virus (EBV) is a ubiquitous human gammaherpesvirus that is carried by the majority of the adult human population as an asymptomatic but persistent infection (1). At the same time, it is one of the most growth-transforming infectious agents and the only one that can readily immortalize its main host cell, the human B

Citation Murer A, Rühl J, Zbinden A, Capaul R, Hammerschmidt W, Chijioko O, Münz C. 2019. MicroRNAs of Epstein-Barr virus attenuate T-cell-mediated immune control *in vivo*. *mBio* 10:e01941-18. <https://doi.org/10.1128/mBio.01941-18>.

Editor Peter Palese, Icahn School of Medicine at Mount Sinai

Copyright © 2019 Murer et al. This is an open-access article distributed under the terms of the [Creative Commons Attribution 4.0 International license](https://creativecommons.org/licenses/by/4.0/).

Address correspondence to Obinna Chijioko, chijioko@immunology.uzh.ch, or Christian Münz, christian.muenz@uzh.ch.

O.C. and C.M. contributed equally to this work.

Received 4 September 2018

Accepted 27 November 2018

Published 15 January 2019

cell, in culture (2). Accordingly, EBV is associated with lymphomas and epithelial cell cancers, which express different subsets of latent EBV gene products. Diffuse large B cell lymphomas and *in vitro*-transformed lymphoblastoid cell lines (LCLs) are positive for six EBV nuclear antigens (EBNAs), two latent membrane proteins (LMPs), two nontranslated Epstein-Barr virus-expressed RNAs (EBERs), and two clusters of microRNAs (miRNAs), the smaller BHRF1 miRNA cluster (3 pre-miRNAs) and the larger BART miRNA cluster (22 pre-miRNAs), giving rise to at least 44 mature miRNAs (3). Only one EBNA (EBNA1) and the two LMPs can be found in classical Hodgkin lymphoma and nasopharyngeal carcinoma, but all nontranslated RNAs are expressed. Finally, Burkitt lymphoma and EBV-associated gastric carcinoma further downregulate latent EBV protein expression and are positive only for EBNA1 but continue to express the nontranslated RNAs. These expression patterns in EBV-associated malignancies are mirrored in B cell differentiation stages of healthy EBV carriers (4). In quiescent memory B cells, EBV protein expression is abolished altogether and only nontranslated EBV RNAs are expressed. This documents the importance of EBERs and viral miRNAs for all latent and growth-transforming stages of EBV infection.

Fortunately, even though all premalignant EBV infection patterns are present in healthy EBV carriers, only a very small fraction of infected individuals develop virus-associated tumors, with an estimated incidence rate of 200,000 new cases of EBV-associated malignancies annually (5). It is thought that the immune system prevents EBV-driven tumor development, because EBV-associated lymphomas occur at increased frequencies in primary and acquired immunodeficiencies (6, 7). Acquired immunodeficiency due to HIV coinfection and primary immunodeficiencies due to mutations in the cytotoxic machinery, lymphocyte costimulation, and T cell receptor signaling identify CD8⁺ T cells as the crucial immune compartments for the control of EBV infection and prevention of associated lymphomagenesis. Accordingly, some EBV-associated tumors can be cured by adoptive transfer of EBV-specific T cell lines (8). Furthermore, in preclinical *in vivo* models of persistent EBV infection, utilizing mice with reconstituted human immune system components (huNSG mice), T cell depletion leads to increased viral loads and lymphoma formation (9–11). EBV seems to strike the right balance, ensuring its persistence after primary infection and allowing sufficient immune control to protect its host. Therefore, it is perhaps not surprising that it has been found *in vitro* that EBV-expressed miRNAs also regulate this T-cell-mediated immune control and dampen antigen presentation on major histocompatibility complex (MHC) class I and II molecules to CD8⁺ and CD4⁺ T cells, respectively (12, 13). However, the importance of this immune evasion by EBV-contained miRNAs remains unclear *in vivo*.

In order to address this question, we explored recombinant Epstein-Barr viruses, lacking either the larger BART cluster of miRNAs or all EBV-expressed miRNAs. In the absence of all EBV miRNAs, the virus established much lower viral titers after infection of huNSG mice. Surprisingly, CD8⁺ T cell depletion restored EBV infection to titers comparable to wild-type virus infection, causing an increase in viral loads by more than 200-fold in the spleen and lymphoma formation in the majority of infected animals. Our findings suggest that EBV-expressed miRNAs mainly serve the purpose of compromising T-cell-mediated immune control and highlight the importance of this immune control in the prevention of EBV-associated lymphoma formation.

RESULTS

EBV infection is attenuated in the absence of viral miRNAs. EBV devoid of its BHRF1 miRNA locus has previously been shown to delay systemic infection in a humanized mouse model without altering the tumor formation capacity of EBV (14). To further investigate the role of EBV miRNA *in vivo*, we used recombinant EBV strains that lack all EBV miRNAs (Δ miR) (15) or only BART miRNAs (Δ miR-BART) to infect NOD-*scid* γ_c^{null} mice with reconstituted human immune system compartments (huNSG mice). Our group and others have previously shown that the huNSG mouse model is a suitable model for EBV infection and cell-mediated immune control *in vivo* (9–11, 16–19). In order to determine the pathogenic potential of Δ miR and Δ miR-BART EBV, we inocu-

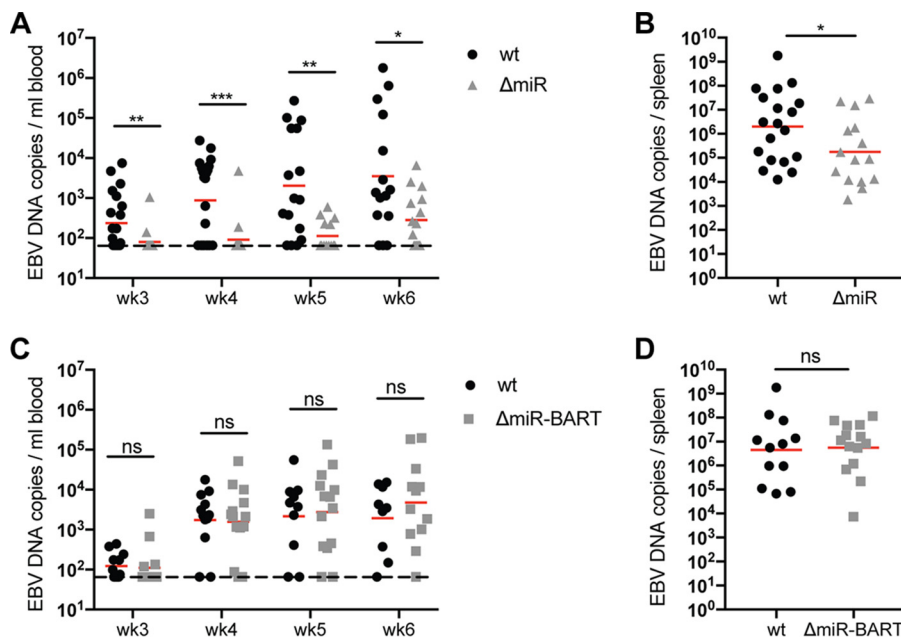


FIG 1 EBV infection is attenuated in the absence of viral miRNAs. (A and C) Blood DNA viral loads over time as determined by qPCR of huNSG mice infected with either wt, Δ miR (A), or Δ miR-BART (C) EBV for 5 to 6 weeks ($n = 14$ to 21/group). The horizontal dashed line indicates the lower limit of quantification (LLOQ). Values below the LLOQ were raised to the LLOQ and plotted on the LLOQ line. (B and D) Splenic endpoint viral DNA loads as determined by qPCR of huNSG mice infected with either wt, Δ miR (B), or Δ miR-BART (D) EBV for 5 to 6 weeks ($n = 12$ to 16/group). (A to D) Pooled data from 4 wt and Δ miR-BART and 6 wt and Δ miR experiments are displayed with geometric mean. *, $P \leq 0.05$; **, $P \leq 0.01$; ***, $P \leq 0.001$, Mann-Whitney U test.

lated huNSG mice with 10^5 Raji-infectious units (RIU) of the respective viruses and monitored infection compared to wild-type (wt) EBV for 5 to 6 weeks. The viral DNA burden was significantly lower in mice infected with Δ miR than with wt EBV, but comparable between Δ miR-BART and wt EBV over the entire observation period in blood, starting at 3 weeks after infection when viral loads became reliably detectable for the first time (Fig. 1A and C), and at the end of the experiments in spleen (Fig. 1B and D). Hence, these data suggest that Δ miR EBV has a reduced, whereas Δ miR-BART EBV has a similar, infectious capacity compared to wt EBV.

Reduced frequencies of proliferating EBV-infected cells in the absence of viral miRNAs. Next, we investigated if the reduced titers of EBV in the absence of its miRNAs are due to decreased proliferation or increased apoptosis. Primary B cells infected with EBV lacking BHRF1 miRNAs were shown to undergo increased apoptotic death and decreased proliferation during the early infection period *in vitro* (15, 20). We therefore examined the frequency of proliferating and apoptotic cells in EBV-infected cells in our *in vivo* system using splenic sections of wt and Δ miR EBV-infected mice. Immunohistochemical analysis of costaining for cleaved caspase 3 (cl. Cas3) and the viral protein EBNA2 suggested that there was less apoptotic activity in Δ miR-infected cells than in wt-infected cells, although this difference did not reach statistical significance (Fig. 2A and B). Overall, the level of cl. Cas3⁺ EBNA2⁺ cells was very low (Fig. 2A). Immunofluorescence costaining for Ki67 and EBNA2 revealed a significantly higher frequency of proliferating EBNA2-positive cells in wt- than in Δ miR-infected mice (Fig. 2C and D). However, established LCLs generated *in vitro* with either wt or Δ miR EBV did not show a growth difference when quantifying total cell numbers over 12 consecutive days (see Fig. S1 in the supplemental material). These results indicate that reduced viral titers in the absence of EBV miRNA might be due to reduced proliferation of infected cells or other factors, such as increased immune control of proliferating infected cells.

Activation and memory formation of CD8⁺ T cells correlate with EBV viral load. Infection of huNSG mice with wt EBV has been reported to induce the activation and

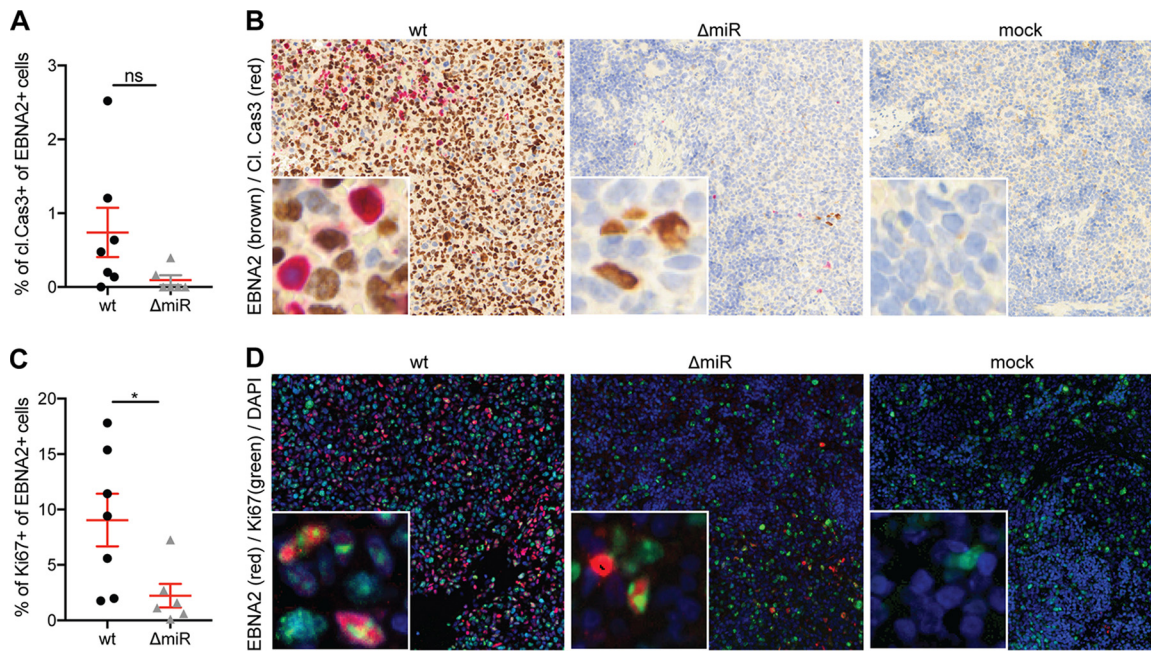


FIG 2 Reduced proliferation of EBV-infected cells in the absence of viral miRNAs. (A and B) Quantification of the frequency of cleaved caspase 3⁺ (cl.Cas3) EBNA2⁺ cells of all EBNA2⁺ cells ($n = 6$ to 7 /group) (A) and representative immunohistochemistry for EBNA2 (brown) and cl.Cas3 (red) (original magnification, $\times 200$) in splenic sections of huNSG mice infected with Δ miR or wt EBV 5 to 6 weeks p.i. or noninfected mice (mock) (B). (C and D) Quantification of the frequency of Ki67⁺ EBNA2⁺ cells of all EBNA2⁺ cells ($n = 6$ to 7 /group) (C) and representative immunofluorescence for EBNA2 (red), Ki67 (green), and DAPI (blue) (original magnification, $\times 200$) in splenic sections of huNSG mice infected with Δ miR or wt EBV 5 to 6 weeks p.i. or mock (D). (A and C) Pooled data from 3 experiments with mean \pm SEM (unpaired t test with Welch's correction).

expansion of human CD8⁺ T cells in huNSG mice (10, 19). Since EBV miRNAs control adaptive antiviral immunity *in vitro* (12, 13), we assessed T cell activation and memory formation upon infection with Δ miR, Δ miR-BART, and wt EBV *in vivo*. In line with the EBV DNA burden in blood and spleen (Fig. 1), we detected similar frequencies of HLA-DR⁺ CD45RO⁺ CD4⁺ T cells (Fig. 3A and Fig. S2A, right panels) and HLA-DR⁺ CD45RO⁺ CD8⁺ T cells (Fig. 3B and Fig. S2B, right panels) in mice infected with wt and Δ miR-BART EBV, whereas mice infected with Δ miR EBV showed reduced frequencies compared to wt EBV 5 to 6 weeks postinfection (p.i.) (Fig. 3A and B, left panels, and Fig. S2A and B, left panels). Investigating specifically the formation of effector or central memory CD8⁺ T cells, frequencies of blood and splenic effector memory (CCR7⁻ CD45RA⁻) CD8⁺ T cells were increased in wt- as well as Δ miR-infected animals compared to noninfected huNSG mice; however, in the absence of EBV miRNAs these frequencies were significantly lower than wt infection (Fig. S3A and C). CCR7⁺ CD45RA⁻ central memory CD8⁺ T cells were increased only in the spleen of wt EBV-infected compared to noninfected mice (Fig. S3B) but not in the blood of wt EBV-infected animals nor in either spleen or blood of Δ miR EBV-infected animals (Fig. S3B and D). The frequency of HLA-DR⁺ CD45RO⁺ CD4⁺ T cells in both blood and spleen did not correlate with EBV DNA loads in the matching organ for any of the infected groups, except in blood for wt-infected mice (Fig. S3C and S2C). In contrast, the frequency of HLA-DR⁺ CD45RO⁺ CD8⁺ T cells in spleen and splenic EBV DNA load correlated significantly for all infection groups (Fig. 3D), while this correlation was absent in the blood (Fig. S2D). This suggests that EBV viral loads primarily drive activated CD8⁺ T cell expansions. Therefore, the observed activation and memory formation of CD8⁺ T cells seem to correlate with EBV DNA burden, which might indicate improved immune control by the less expanded CD8⁺ T cells during Δ miR infection or decreased CD8⁺ T cell expansion due to lower antigenic load.

Proliferation and LCL-specific cytokine production of CD8⁺ T cells are lower in Δ miR than wt EBV-infected mice, whereas cytolytic granule contents of CD8⁺ T

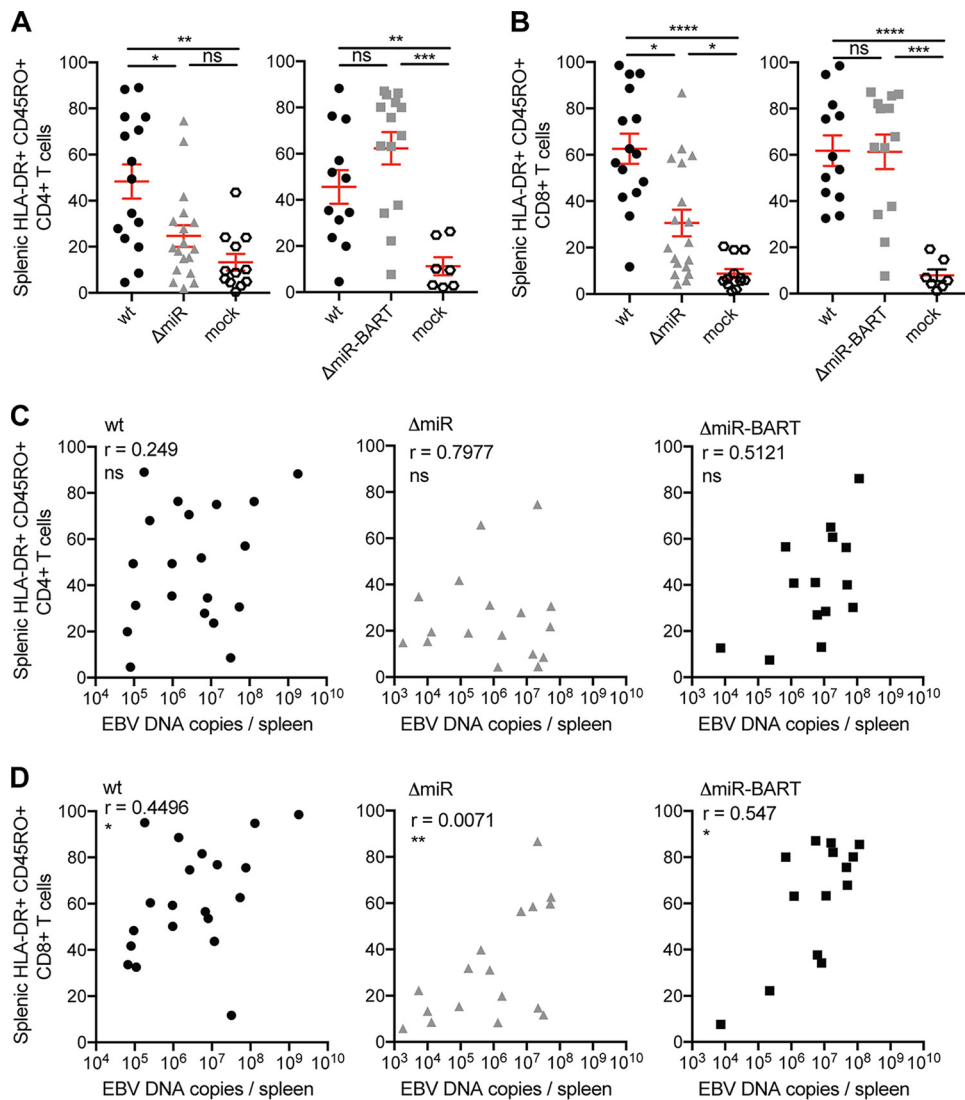


FIG 3 Activation and memory formation of CD8⁺ T cells correlate with EBV viral load. (A and B) The frequency of splenic HLA-DR⁺ CD45RO⁺ CD4⁺ T cells (A) and splenic HLA-DR⁺ CD45RO⁺ CD8⁺ T cells (B) of huNSG mice infected with either 10⁵ RIU of wt, ΔmiR, or ΔmiR-BART EBV 5 to 7 weeks p.i. or mock huNSG mice ($n = 7$ to 18/group) was determined by flow cytometry. (C and D) Correlation of the frequencies of activated memory CD4⁺ (C) and activated memory CD8⁺ (D) T cells, from panels A and C, respectively, with the splenic endpoint viral DNA loads as determined by qPCR for each infected group. (A and B) Pooled data from 4 wt and ΔmiR-BART and 5 wt and ΔmiR experiments with mean \pm SEM. *, $P \leq 0.05$; **, $P \leq 0.01$; ***, $P \leq 0.001$; ****, $P \leq 0.0001$, Mann-Whitney U test. (C and D) Pooled data from 4 to 7 experiments. *, $P \leq 0.05$; **, $P \leq 0.01$, Spearman correlation.

cells seem similar in the two infectious groups. To investigate the immune response to EBV more thoroughly, we examined Ki67 and perforin expression in CD8⁺ T cells on splenic sections of infected huNSG mice. The frequency of CD8⁺ T cells positive for the cytolytic effector molecule perforin was significantly increased in wt but not in ΔmiR EBV-infected mice compared to noninfected controls, whereas no significant difference between wt and ΔmiR EBV-infected mice was observed (Fig. 4A and B, left panels). Nevertheless, we detected a significantly higher frequency of proliferating CD8⁺ cells in wt EBV-infected than ΔmiR EBV-infected mice or noninfected controls (Fig. 4A and B, right panels). Additionally, we assessed EBV-specific T cell responses by coculturing CD19⁻ splenocytes with autologous LCLs generated with wt EBV and analyzed IFN- γ release by ELISpot assay. Cocultures containing splenocytes isolated from wt-infected mice showed significantly increased EBV-specific T cell reactivity compared to cocultures with splenocytes from ΔmiR-infected or mock-infected mice (Fig. 4C). However,

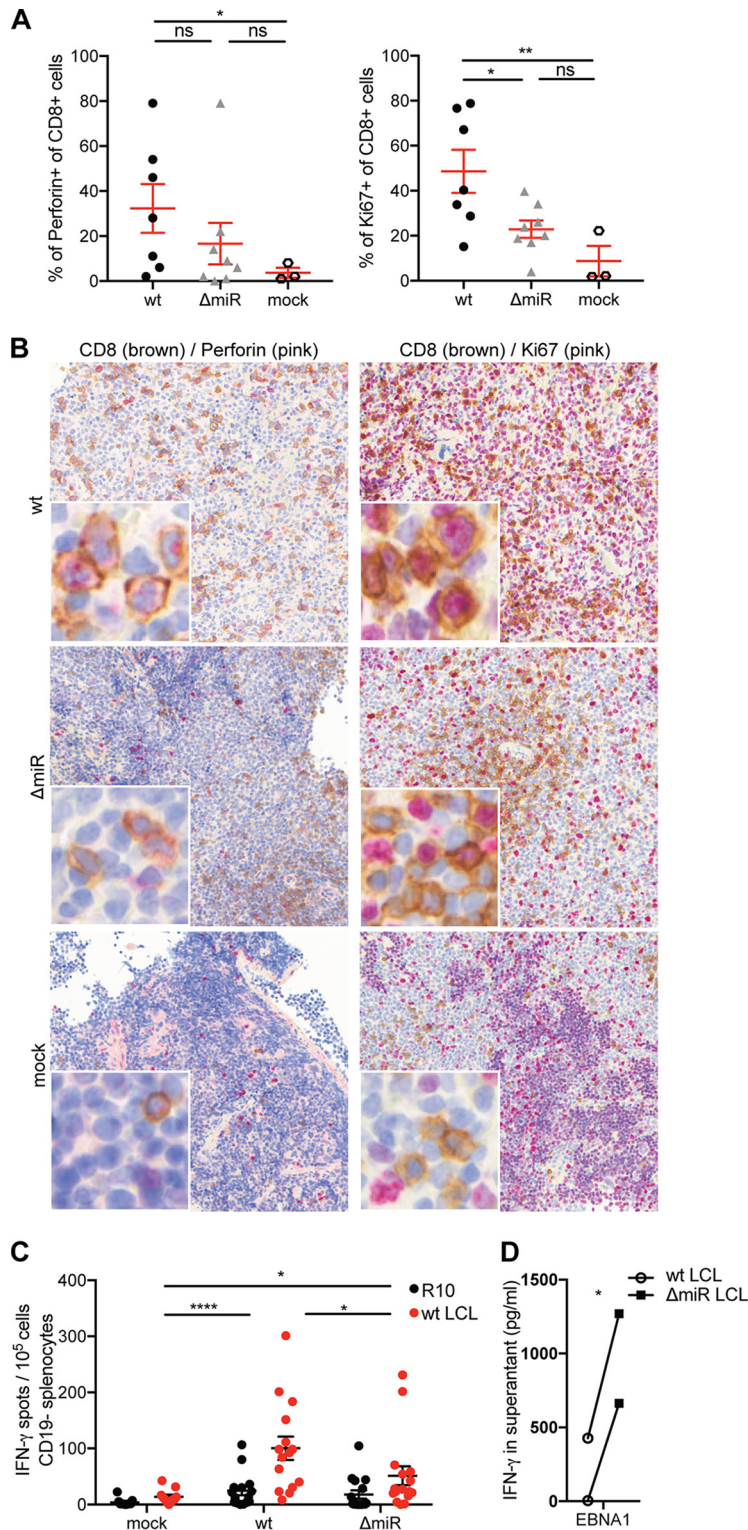


FIG 4 Proliferation and LCL-specific cytokine production of CD8⁺ T cells are lower in ΔmiR than wt EBV-infected mice, whereas cytolytic granule contents of CD8⁺ T cells seem similar in the two infectious groups. (A and B) Quantitation of the frequency of perforin⁺ CD8⁺ cells of all CD8⁺ cells or Ki67⁺ CD8⁺ cells of all CD8⁺ cells ($n = 3$ to 8/group) (A) and the representative immunohistochemistry staining with CD8 (brown) and perforin (pink) (left column; original magnification, $\times 200$) or CD8 (brown) and Ki67 (pink) (right column; original magnification, $\times 200$) in splenic sections of huNSG mice infected with either ΔmiR or wt EBV 5 to 6 weeks p.i. or mock huNSG mice (B). (C) Evaluation of the EBV-specific T cell response through the measurement of the IFN- γ release via ELISpot assay upon coculture of CD19⁻ splenocytes, derived from ΔmiR or wt EBV-infected or noninfected (mock) huNSG mice, with autologous (Continued on next page)

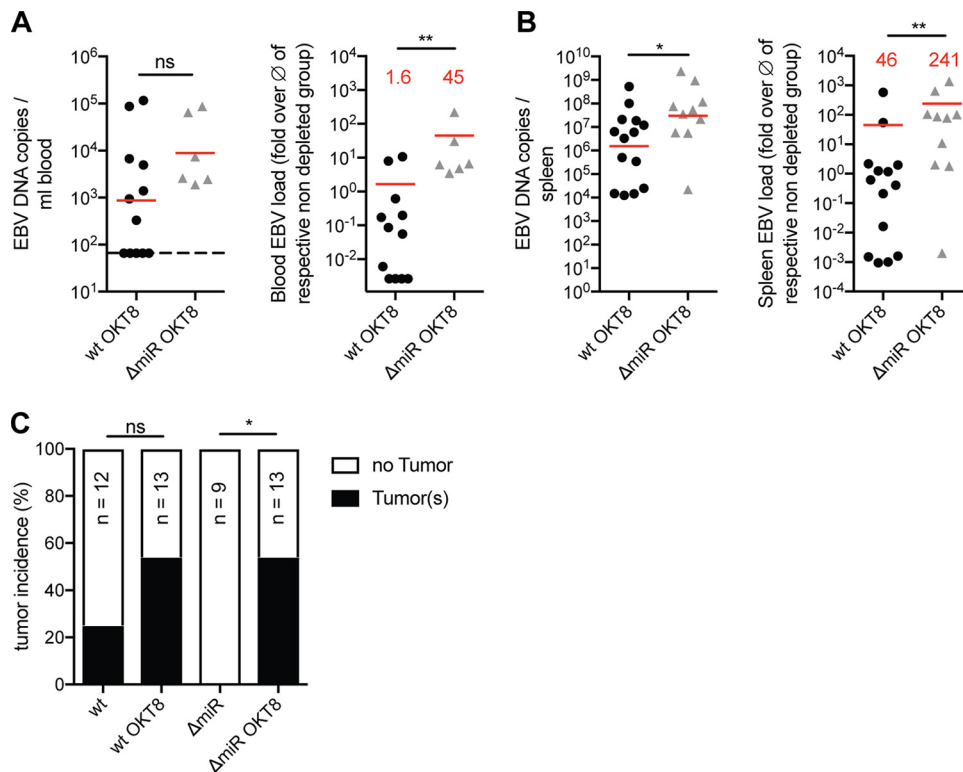


FIG 5 CD8 depletion rescues impaired viral infectious capacity of EBV devoid of its miRNAs. (A and B) Blood (A) and spleen (B) DNA viral loads determined by qPCR of huNSG mice ($n = 5$ to 14 /group) infected with either wt or Δ miR EBV and treated with OKT8 for CD8⁺ T cell depletion (left) or the matching relative viral loads normalized to the mean of the corresponding nondepleted groups ($n = 8$ to 12 /group) with the indication of the fold difference (red) for the different infection groups (right) 5 weeks p.i. (A) Horizontal dashed line indicates the lower limit of quantification (LLOQ). Values below the LLOQ were raised to the LLOQ and plotted on the LLOQ line. (C) Frequency of tumor formation observed in mice infected with wt or Δ miR EBV nontreated or treated with OKT8. (A and B) Pooled data from 4 experiments with geometric mean (left) and arithmetic mean (right). *, $P \leq 0.05$; **, $P \leq 0.01$, Mann-Whitney U test. (C) Pooled data from 4 experiments. *, $P \leq 0.05$, Fisher's exact test.

splenocytes from Δ miR-infected mice still produced significantly more IFN- γ spots than cells from noninfected mice (Fig. 4C). Thus, EBV-specific T cell responses were detected in all infected groups but were higher in wt than in Δ miR EBV-infected mice. Nevertheless, as shown in a previous study (12), we found increased IFN- γ release when coculturing EBV-specific CD8⁺ T cell clones with autologous Δ miR LCL compared to coculture with wt LCLs (Fig. 4D). This suggests that the less expanded CD8⁺ T cell compartment might control Δ miR EBV-infected B cells more efficiently; even so, miRNA-deficient EBV infection induces less T cell proliferation, thereby accumulating fewer cytolytic granule-containing and cytokine-producing CD8⁺ T cells *in vivo*.

CD8 depletion rescues impaired infectious capacity of EBV devoid of its miRNAs. In order to address the T-cell-mediated immune control of Δ miR EBV infection more specifically, we depleted CD8⁺ T cells with OKT8 antibodies before and during the infection of huNSG mice with wt or Δ miR EBV. Depletion of CD8⁺ T cells led to similar or even increased EBV loads in Δ miR EBV-infected compared to wt EBV-infected huNSG mice (Fig. 5A and B, left panels). Normalizing the viral loads to infected mice not treated with OKT8 antibodies revealed that the fold increases over the average of the matching

FIG 4 Legend (Continued)

wt LCLs or medium (R10). (D) Assessment of the IFN- γ release via ELISA upon coculture of Δ miR or wt LCL with an EBNA1-specific CD8⁺ T cell clone for 16 h. (A) Pooled data from 3 experiments represented with the mean \pm SEM (*, $P \leq 0.05$; **, $P \leq 0.01$, unpaired *t* test with Welch's correction). (C) Pooled data from 5 experiments represented with the mean \pm SEM (*, $P \leq 0.05$; ****, $P \leq 0.0001$, Mann-Whitney U test). (D) Data from 2 experiments (*, $P \leq 0.05$, paired *t* test).

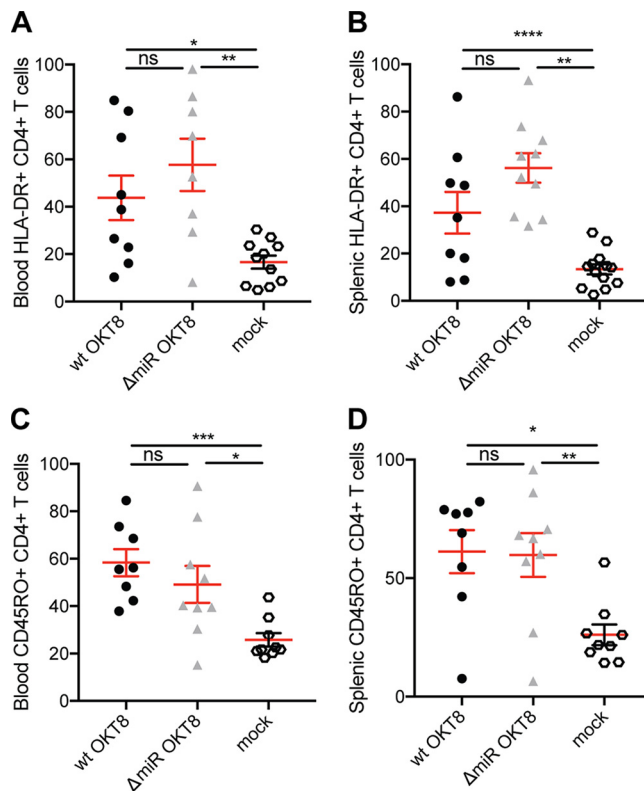


FIG 6 Absence of CD8⁺ T cells alters CD4⁺ T cell recognition of EBV without viral miRNAs. The frequencies of blood (A) and splenic (B) HLA-DR⁺ CD4⁺ T cells and of blood (C) and splenic (D) CD45RO⁺ CD4⁺ T cells of huNSG mice infected with either wt or ΔmiR EBV treated with OKT8 for CD8⁺ T cell depletion 5 weeks p.i. ($n = 3$ to 13/group) as determined by flow cytometry. (A to D) Pooled data from 2 to 3 experiments with mean \pm SEM. *, $P \leq 0.05$; **, $P \leq 0.01$; ***, $P \leq 0.001$; ****, $P \leq 0.0001$, Mann-Whitney U test.

nondepleted groups were significantly higher, up to 240-fold, in the ΔmiR- compared to wt-infected animals in blood and spleen (Fig. 5A and B, right panels). Hence, ΔmiR EBV seems to be better controlled by CD8⁺ T cells *in vivo* than wt EBV. Furthermore, although ΔmiR EBV infection in huNSG mice never induced tumor formation in the presence of an unmanipulated T cell compartment, upon OKT8 treatment tumor incidence reached levels comparable to wt EBV-infected mice (Fig. 5C). Thus, these data suggest that EBV miRNAs are able to reduce immune surveillance by T cells *in vivo*.

Absence of CD8⁺ T cells alters CD4⁺ T cell recognition of miRNA-deficient EBV.

Since reduced frequencies of HLA-DR⁺ CD45RO⁺ T cells were observed in ΔmiR compared to wt EBV-infected huNSG mice, we aimed to investigate whether the absence of CD8⁺ T cells changed CD4⁺ T cell activation and memory formation. Specifically, we explored HLA-DR and CD45RO expression on CD4⁺ T cells. In both blood and spleen, there was a trend toward higher frequencies of activated HLA-DR⁺ CD4⁺ T cells in ΔmiR compared to wt EBV-infected mice treated with OKT8, though no significant differences were observed (Fig. 6A and B). However, the frequency of memory CD45RO⁺ CD4⁺ T cells seemed comparable between ΔmiR- and wt-infected mice inoculated with OKT8 (Fig. 6C and D). Nevertheless, we observed higher frequencies of blood and splenic HLA-DR⁺ CD4⁺ T cells (Fig. 6A and B) and higher frequencies of blood and splenic CD45RO⁺ CD4⁺ T cells in OKT8-treated wt and ΔmiR EBV-infected mice compared to noninfected mice (Fig. 6C and D). Thus, the immune response to ΔmiR EBV seems to generate a slightly higher activation and comparable memory formation in the remaining T cells when depleted for CD8⁺ T cells, suggesting that CD4⁺ T cells might also be more efficiently activated by ΔmiR EBV-infected cells.

DISCUSSION

EBV was among the first viruses which were described to express miRNAs (21, 22). A wide spectrum of cellular, host, and viral functions have been described to be regulated by at least 44 mature miRNAs that EBV expresses (3, 23). Our *in vivo* model of EBV infection in huNSG mice now reveals that the main outcome of loss of miRNA expression is elevated T-cell-mediated immune control of viral infection and associated tumorigenesis. This improved immune control is associated with decreased numbers of proliferating EBV-infected B cells and attenuated T cell expansion. Consistent with a previous study that already demonstrated delayed kinetics of EBV infection and a tendency toward lower virus-associated lymphomagenesis in the absence of the BHRF1 miRNAs (14), we also find reduced viral loads and no detectable tumorigenesis with the complete miRNA-deficient virus but unchanged infection with BART miRNA knockout EBV. Furthermore, deletion of the EBERs, another prominent species of EBV-expressed nontranslated RNAs, has also no significant effect on EBV infection in huNSG mice (24). This suggests that the BHRF1 miRNAs influence viral infection and tumor formation more strongly than EBERs or the BART miRNAs, and this regulation mainly affects T cell recognition.

Immune evasion by miRNAs affects all stages of the EBV life cycle because it also covers the latent EBV infection programs that are important for the virus to persist, while most of the immune evasive proteins encoded by the virus are expressed only during lytic replication. These fall into four categories, inhibiting immune sensing via Toll-like receptors (TLRs) and the downstream NF- κ B activation, compromising the type I IFN response, downregulating MHC-restricted antigen presentation, and changing a pro- into an anti-inflammatory environment (25). For example, BGLF5 and BPLF1 downregulate TLRs or interfere with TLR-mediated NF- κ B activation (26, 27). Furthermore, BZLF1, BRLF1, BILF1, and BGLF4 reduce expression or inhibit the function of interferon-responsive factors (IRFs) 3 and 7 to compromise type I IFN responses (28–31). EBV also encodes BNLF2a, a protein that blocks peptide import into the endoplasmic reticulum (ER) via the transporter associated with antigen presentation (TAP) (32–35); BILF1, a protein that reduces MHC class I surface levels (34, 36, 37); BZLF2, a protein that interferes with T cell receptor binding to MHC class II (38, 39); and BDLF3, a protein that shields MHC class I- and II-restricted antigen presentation from T cell recognition (40). Finally, EBV-infected cells secrete a soluble macrophage colony-stimulating factor (M-CSF) receptor that is encoded in the BARF1 gene (41, 42) and viral IL-10 from the BCRF1 gene (43), which reduce inflammation and thereby immune surveillance of infected cells. In contrast, latent EBV proteins mainly diminish their own antigen presentation *in cis*, by limiting their protein expression and/or actively inhibiting their proteasomal degradation, as is the case for EBNA1 (44, 45). Thus, virally encoded proteins contribute to immune evasion *in trans* mainly during lytic EBV replication, while nontranslated miRNAs might primarily serve this purpose during latent EBV infection.

For this purpose, EBV miRNAs attenuate viral antigen production, compromise MHC class I-restricted antigen presentation via TAP downregulation and MHC class II-restricted antigen presentation via inhibition of lysosomal degradation, and diminish production of the T cell chemoattractant CXCL11 and the T-cell-priming cytokine IL-12 (3). For antigen recognition by CD8⁺ T cells, primarily TAP2 mRNA downregulation and targeting by the RNA-induced silencing complex (RISC) have been identified as viral miRNA targets (12). This diminishes also TAP1 protein levels as well as surface expression of especially HLA-B molecules, which are the main MHC class I restriction elements of immunodominant EBV-specific CD8⁺ T cell responses (46). Even though our T cell depletion experiments clearly argue that such miRNA functions dominate the outcome of EBV infection at week 5 with respect to viral loads and tumor formation, other previously *in vitro*-defined functions of EBV miRNAs might be responsible for the lower viral loads that we detect already at week 3 after infection. At this 3-week time point, lytic replication contributes to viral loads in our *in vivo* model of EBV infection, as could be demonstrated by comparing wild-type with lytic-replication-deficient (BZLF1 knockout) virus (16). Along these lines, sumoylation seems to be required for infectious virus production, and the SUMO ligase RNF4 is downregulated by the BHRF1-1 miRNA (47).

This could suggest that diminished lytic EBV replication could contribute to the lower viral loads at week 3 after infection. Furthermore, BHRF1 miRNAs of EBV have been suggested to be required for efficient B cell transformation by attenuating viral protein expression (20, 48). They seem to optimize the expression timing of EBNA-LP and BHRF1, a viral antiapoptotic Bcl-2 homologue, in *cis*, when they get processed from the transcripts of these viral proteins that also contain their pri-miRNAs (49, 50). Also, these mechanisms might contribute to the diminished viral loads upon miRNA-deficient EBV infection in huNSG mice at early time points after infection. However, these defects seemed to be transient *in vitro*, and no growth defects could be detected in established EBV-transformed B cell lines. Similarly, in our studies at 5 weeks postinfection miRNA-mediated attenuation of T cell responses predominated and viral loads as well as tumor formation by Δ miR EBV could be restored by T cell depletion. Thus, miRNA deficiency could be further explored to promote immune responses with an attenuated EBV that might be considered for prophylactic vaccination against symptomatic primary infection, i.e., infectious mononucleosis.

MATERIALS AND METHODS

Recombinant EBV. Concentrates of the green fluorescent protein (GFP)-encoding Epstein-Barr virus (EBV) miRNA knockout (Δ miR, p4027), EBV BART miRNA knockout (Δ miR-BART, p5446), or EBV wild-type (wt, p2089) viruses were prepared as previously described (12, 13, 51) and titrated on Raji cells. The miRNA-expressing loci in the Δ miR and Δ miR-BART viruses were replaced with computed scrambled sequences as described previously (15). The GFP-expressing cells were quantified by flow cytometry 2 days later to calculate Raji-infecting units (RIU). For *in vitro* infection of B cells, B cells isolated from splenocytes or human PBMCs were isolated using anti-CD19 microbeads (Miltenyi Biotec) and infected with wt or Δ miR EBV with the addition of a CD40L-expressing feeder cell line irradiated with 140 Gy. The cells were maintained in RPMI 1640 medium (Gibco, Thermo Fisher Scientific) with 10% FCS, streptomycin, and penicillin in the absence of the CD40L-expressing feeder cell line. Total numbers of established LCLs were determined by trypan blue staining.

Mice with reconstituted human immune system components and infection with EBV. NOD-*scid* γ_c^{null} (NSG) mice and HLA-A2 transgenic NSG mice were obtained from the Jackson Laboratories and maintained under specific-pathogen-free conditions. Reconstitution was performed as previously described (52). Reconstitution level was checked 10 to 12 weeks later and again a week prior to the start of the experiments by flow cytometric immune phenotyping of peripheral blood as previously described (16). Mice were infected intraperitoneally with 1×10^5 RIU of wt, Δ miR, or Δ miR-BART EBV and followed for 5 or 6 weeks. Samples below the lower limit of quantification (LLOQ) of 67 EBV DNA copies were considered negative for EBV DNA. The value of the LLOQ was used for the blood DNA copies of mice having a viral load in the spleen but not in the blood. Mice without any viral loads in the blood and spleen throughout the experiment were considered not infected and excluded from the analysis.

Purification of mouse anti-human CD8 antibody. OKT8 hybridoma cells (mouse IgG2a; ATCC, Manassas, VA, USA) were gradually adapted to serum- and protein-free PFHM-II medium (Thermo Fisher Scientific [formerly Gibco], catalog no. 12040-077). Cells were cultured in BD CELLline 1000 flasks (BD catalog no. 353137) according to the manufacturer's recommendation. Antibodies were precipitated from the culture supernatant by addition of an equal volume of saturated ammonium-sulfate solution. After buffer exchange to PBS using PD-10 desalting columns (Sephadex G25 medium; GE Healthcare), antibodies were sterilized by filtration through 0.2- μ m filters (Filtropur S 0.2; Sarstedt) and stored at 4°C until use.

Depletion of T cells. Human CD8⁺ T cells were depleted in mice before EBV infection by intraperitoneal injection of 100 μ g OKT8 antibodies on three consecutive days. To deplete T cells for the duration of the experiment, 50 μ g of the depletion antibodies was injected 3 times a week starting 2 weeks postinfection until the day of sacrifice.

Quantification of viral load. DNA from splenic tissue was obtained using a QIAamp DNA tissue kit (Qiagen) and from whole blood using the NucliSENS EasyMAG System (bioMérieux), both according to the manufacturers' recommendations. The TaqMan (Applied Biosystems) real-time PCR technique was performed to quantitatively analyze EBV DNA as previously described (53), with modified primers for the BamHI W fragment (5'-CTTCTCAGTCCAGCGCGTTT-3' and 5'-CAGTGGTCCCTCCCTAGA-3') and a fluorogenic probe (5'-FAM-CGTAAGCCAGACAGCAGCCAATTGTCAG-TAMRA-3'). All PCRs were run on an ABI Prism 7300 Sequence Detector or ViiA7-240 Real-Time PCR system (Applied Biosystems), and samples were analyzed in duplicate.

Flow cytometry. All fluorescently labeled antibodies are listed in Table S1 in the supplemental material. Lysis of erythrocytes in whole blood was done with NH_4Cl . Spleens were mashed and filtered through a 70- μ m cell strainer before separation of mononuclear cells on Ficoll-Paque gradients. Cell suspensions were stained with antibodies for 30 min at 4°C, washed, and analyzed on FACS Canto or LSR Fortessa cytometers (BD Biosciences). Analysis of flow cytometric data was performed with FlowJo (Tree Star).

Histology, immunohistochemistry, and immunofluorescence. Tissue was fixed in 10% saline-buffered formalin and paraffin embedded. For immunohistochemistry and immunofluorescence, 3- μ m sections were processed on a Leica Bond-Max or Bond-III automated immunohistochemistry system. Stainings were performed with monoclonal mouse anti-EBNA2 (clone PE2; Abcam), rabbit anti-Ki67

(clone SP6; Cell Marque), rabbit anti-huCD8 (clone SP16; Marque), mouse antiperforin (5B10; Novocastra Laboratories), and polyclonal cleaved caspase 3 (Cell Signaling Technology). For immunofluorescence, the AF488 donkey anti-rabbit IgG (Jackson ImmunoResearch), DyLight549 horse anti-mouse IgG (Vectrolabs), and DAPI (Sigma) were used. Stainings were analyzed as described elsewhere (52) using the Vectra3 automated quantitative pathology imaging system (PerkinElmer) and InForm software analysis (PerkinElmer). The percentage of EBNA2 plus Ki67, EBNA2 plus cleaved caspase 3, huCD8 plus Ki67, or huCD8 plus perforin double-positive cells of all EBNA2- or huCD8-positive cells was calculated.

EBV-specific IFN- γ release assay (ELISpot). EBV-specific T cell responses were analyzed using an IFN- γ enzyme-linked immunospot (ELISpot) assay as previously described (10, 54). Briefly, splenocytes were depleted of human CD19⁺ cells using anti-CD19 microbeads (Miltenyi Biotec). The CD19-depleted fraction was stimulated with autologous LCLs at a ratio of 1:4 for 18 h, and incubation with R10 and phorbol myristate acetate (PMA)-ionomycin served as negative and positive controls, respectively. Each condition was performed in duplicates. Spots were counted on an ELISpot reader system (ELRO2; Autoimmun Diagnostika GmbH).

CD8⁺ T cell cloning and restimulation. CD8⁺ T cell clones specific for the nuclear antigen 1 of EBV (EBNA1) were generated from freshly isolated PBMCs which were depleted of CD4⁺ T cells using anti-CD4-conjugated MACS microbeads and magnetic selection (Miltenyi Biotec). PBMCs were stimulated with 5 μ M EBNA1-derived HPVGEADYFEY peptide (aa 407 to 417) for 3 to 4 h. Responding cells were enriched by IFN- γ secretion assay (130-054-201; Miltenyi Biotec) and were cloned by limiting dilution at 3 and 30 cells per well on HLA-matched irradiated LCLs (10⁴/well) loaded with the relevant peptide at 5 μ M and allogeneic irradiated, PHA-treated PBMCs (10⁵/well) in medium with 10% pooled human sera supplemented with 150 IU/ml IL-2 (T cell medium). Growing microcultures were screened for peptide reactivity by IFN- γ ELISA (3420-1H-20; Mabtech). Selected CD8⁺ T cell clones were further expanded on autologous irradiated LCLs loaded with the relevant peptide at 5 μ M and allogeneic irradiated, PHA-treated PBMCs in T cell medium. Clones were maintained in T cell medium. Every 2 to 3 weeks, CD8⁺ T cell clones were restimulated with peptide-pulsed autologous LCLs and allogeneic PHA-treated PBMCs. The resulting CD8⁺ T cell clone used in this study was specific for EBNA1₄₀₇₋₄₁₇ (HPVGEADYFEY, HLA-B*3501). To investigate specific recognition of target cells, 10,000 CD8⁺ T cell clones were cocultured with 100,000 autologous wt or Δ miR LCLs. After overnight incubation, coculture supernatants from single wells were tested by ELISA for IFN- γ content.

Statistical analysis. Statistical analysis and graph preparation were performed with Prism software (GraphPad). A paired *t* test, unpaired *t* test with Welch's correction, or two-tailed Mann-Whitney U test was used. A *P* value of <0.05 was considered statistically significant.

Study approval. All animal protocols were approved by the cantonal veterinary office of the canton of Zürich, Switzerland (protocols 209/2014 and 159/2017). All studies involving human samples were reviewed and approved by the cantonal ethics committee of Zürich, Switzerland (protocol KEK-StV-Nr.19/08).

SUPPLEMENTAL MATERIAL

Supplemental material for this article may be found at <https://doi.org/10.1128/mBio.01941-18>.

FIG S1, TIF file, 0.1 MB.

FIG S2, TIF file, 1 MB.

FIG S3, TIF file, 0.4 MB.

TABLE S1, DOCX file, 0.1 MB.

ACKNOWLEDGMENTS

This study was supported by Cancer Research Switzerland (KFS-4091-02-2017 and KLS-4231-08-2017); KFSP^{MS}, KFSP-Precision^{MS}, and KFSP^{HLLD} of the University of Zurich; the Vontobel Foundation; the Baugarten Foundation; the Sobek Foundation; the Swiss Vaccine Research Institute; the Swiss MS Society; and the Swiss National Science Foundation (310030_162560 and CRSII3_160708). W.H. was supported by the Deutsche Forschungsgemeinschaft (grant number SFB1064/TP A04) and the Deutsche Krebshilfe (grant numbers 107277 and 109661) and by grants from the German Centre for Infection Research (DZIF) (07.803 and 07.906).

REFERENCES

- Young LS, Yap LF, Murray PG. 2016. Epstein-Barr virus: more than 50 years old and still providing surprises. *Nat Rev Cancer* 16:789–802. <https://doi.org/10.1038/nrc.2016.92>.
- Cesarman E. 2014. Gammaherpesviruses and lymphoproliferative disorders. *Annu Rev Pathol* 9:349–372. <https://doi.org/10.1146/annurev-pathol-012513-104656>.
- Albanese M, Tagawa T, Buschle A, Hammerschmidt W. 2017. MicroRNAs of Epstein-Barr virus control innate and adaptive antiviral immunity. *J Virol* 91:e01667-16. <https://doi.org/10.1128/JVI.01667-16>.
- Babcock GJ, Hochberg D, Thorley-Lawson DA. 2000. The expression pattern of Epstein-Barr virus latent genes in vivo is dependent upon the differentiation stage of the infected B cell. *Immunity* 13:497–506. [https://doi.org/10.1016/S1074-7613\(00\)00049-2](https://doi.org/10.1016/S1074-7613(00)00049-2).
- Cohen JI, Fauci AS, Varmus H, Nabel GJ. 2011. Epstein-Barr virus: an

- important vaccine target for cancer prevention. *Sci Transl Med* 3: 107fs7. <https://doi.org/10.1126/scitranslmed.3002878>.
6. Tangye SG, Palendira U, Edwards ESJ. 2017. Human immunity against EBV—lessons from the clinic. *J Exp Med* 214:269–283. <https://doi.org/10.1084/jem.20161846>.
 7. Totonchy J, Cesarman E. 2016. Does persistent HIV replication explain continued lymphoma incidence in the era of effective antiretroviral therapy? *Curr Opin Virol* 20:71–77. <https://doi.org/10.1016/j.coviro.2016.09.001>.
 8. McLaughlin LP, Gottschalk S, Rooney CM, Bollard CM. 2017. EBV-directed T cell therapeutics for EBV-associated lymphomas. *Methods Mol Biol* 1532:255–265. https://doi.org/10.1007/978-1-4939-6655-4_19.
 9. Chijioke O, Marcenaro E, Moretta A, Capaul R, Münz C. 2015. Role of the 2B4 receptor in CD8⁺ T-cell-dependent immune control of Epstein-Barr virus infection in mice with reconstituted human immune system components. *J Infect Dis* 212:803–807. <https://doi.org/10.1093/infdis/jiv114>.
 10. Strowig T, Gurer C, Ploss A, Liu YF, Arrey F, Sashihara J, Koo G, Rice CM, Young JW, Chadburn A, Cohen JI, Münz C. 2009. Priming of protective T cell responses against virus-induced tumors in mice with human immune system components. *J Exp Med* 206:1423–1434. <https://doi.org/10.1084/jem.20081720>.
 11. Yajima M, Imadome K, Nakagawa A, Watanabe S, Terashima K, Nakamura H, Ito M, Shimizu N, Yamamoto N, Fujiwara S. 2009. T cell-mediated control of Epstein-Barr virus infection in humanized mice. *J Infect Dis* 200:1611–1615. <https://doi.org/10.1086/644644>.
 12. Albanese M, Tagawa T, Bouvet M, Maliqi L, Lutter D, Hoser J, Hastreiter M, Hayes M, Sugden B, Martin L, Moosmann A, Hammerschmidt W. 2016. Epstein-Barr virus microRNAs reduce immune surveillance by virus-specific CD8⁺ T cells. *Proc Natl Acad Sci U S A* 113:E6467–E6475. <https://doi.org/10.1073/pnas.1605884113>.
 13. Tagawa T, Albanese M, Bouvet M, Moosmann A, Mautner J, Heissmeyer V, Zielinski C, Lutter D, Hoser J, Hastreiter M, Hayes M, Sugden B, Hammerschmidt W. 2016. Epstein-Barr viral miRNAs inhibit antiviral CD4⁺ T cell responses targeting IL-12 and peptide processing. *J Exp Med* 213:2065–2080. <https://doi.org/10.1084/jem.20160248>.
 14. Wahl A, Linnstaedt SD, Esoda C, Krisko JF, Martinez-Torres F, Delecluse H-J, Cullen BR, Garcia JV. 2013. A cluster of virus-encoded microRNAs accelerates acute systemic Epstein-Barr virus infection but does not significantly enhance virus-induced oncogenesis in vivo. *J Virol* 87: 5437–5446. <https://doi.org/10.1128/JVI.00281-13>.
 15. Seto E, Moosmann A, Grömminger S, Walz N, Grundhoff A, Hammerschmidt W. 2010. MicroRNAs of Epstein-Barr virus promote cell cycle progression and prevent apoptosis of primary human B cells. *PLoS Pathog* 6:e1001063. <https://doi.org/10.1371/journal.ppat.1001063>.
 16. Antsiferova O, Müller A, Rämmer P, Chijioke O, Chatterjee B, Raykova A, Planas R, Sospedra M, Shumilov A, Tsai MH, Delecluse HJ, Münz C. 2014. Adoptive transfer of EBV specific CD8⁺ T cell clones can transiently control EBV infection in humanized mice. *PLoS Pathog* 10:e1004333. <https://doi.org/10.1371/journal.ppat.1004333>.
 17. Ma SD, Xu X, Plowshay J, Ranheim EA, Burlingham WJ, Jensen JL, Asimakopoulou F, Tang W, Gulley ML, Cesarman E, Gumperz JE, Kenney SC. 2015. LMP1-deficient Epstein-Barr virus mutant requires T cells for lymphomagenesis. *J Clin Invest* 125:304–315. <https://doi.org/10.1172/JCI76357>.
 18. Yajima M, Imadome K, Nakagawa A, Watanabe S, Terashima K, Nakamura H, Ito M, Shimizu N, Honda M, Yamamoto N, Fujiwara S. 2008. A new humanized mouse model of Epstein-Barr virus infection that reproduces persistent infection, lymphoproliferative disorder, and cell-mediated and humoral immune responses. *J Infect Dis* 198:673–682. <https://doi.org/10.1086/590502>.
 19. Chijioke O, Müller A, Feederle R, Barros MHM, Krieg C, Emmel V, Marcenaro E, Leung CS, Antsiferova O, Landtwin V, Bossart W, Moretta A, Hassan R, Boyman O, Niedobitek G, Delecluse H-J, Capaul R, Münz C. 2013. Human natural killer cells prevent infectious mononucleosis features by targeting lytic Epstein-Barr virus infection. *Cell Rep* 5:1489–1498. <https://doi.org/10.1016/j.celrep.2013.11.041>.
 20. Feederle R, Linnstaedt SD, Bannert H, Lips H, Bencun M, Cullen BR, Delecluse H-J. 2011. A viral microRNA cluster strongly potentiates the transforming properties of a human herpesvirus. *PLoS Pathog* 7:e1001294. <https://doi.org/10.1371/journal.ppat.1001294>.
 21. Pfeffer S, Zavolan M, Grässer FA, Chien H, Russo JJ, Ju J, John B, Enright AJ, Marks D, Sander C, Tuschl T. 2004. Identification of virus-encoded microRNAs. *Science* 304:734–737. <https://doi.org/10.1126/science.1096781>.
 22. Pfeffer S, Sewer A, Lagos-Quintana M, Sheridan R, Sander C, Grässer FA, van Dyk LF, Kiong Ho C, Shuman S, Chien M, Russo JJ, Ju J, Randall G, Linderbach BD, Rice CM, Simon V, Ho DD, Zavolan M, Tuschl T. 2005. Identification of microRNAs of the herpesvirus family. *Nat Methods* 2:269–276. <https://doi.org/10.1038/nmeth746>.
 23. Skalsky RL, Cullen BR. 2015. EBV noncoding RNAs. *Curr Top Microbiol Immunol* 391:181–217. https://doi.org/10.1007/978-3-319-22834-1_6.
 24. Gregorovic G, Boulden EA, Bosshard R, Karstegl E, Skalsky R, Cullen BR, Gujer C, Rämmer P, Münz C, Farrell J. 2015. Epstein-Barr viruses (EBVs) deficient in EBV-encoded RNAs have higher levels of latent membrane protein 2 RNA expression in lymphoblastoid cell lines and efficiently establish persistent infections in humanized mice. *J Virol* 89: 11711–11714. <https://doi.org/10.1128/JVI.01873-15>.
 25. Rensing ME, Van Gent M, Gram AM, Hooykaas MJG, Piersma SJ, Wiertz EJHJ. 2015. Immune evasion by Epstein-Barr virus. *Curr Top Microbiol Immunol* 391:355–381. https://doi.org/10.1007/978-3-319-22834-1_12.
 26. van Gent M, Braem SGE, de Jong A, Delagic N, Peeters JGC, Boer IGJ, Moynagh PN, Kremmer E, Wiertz EJ, Ovaa H, Griffin BD, Rensing ME. 2014. Epstein-Barr virus large tegument protein BPLF1 contributes to innate immune evasion through interference with Toll-like receptor signaling. *PLoS Pathog* 10:e1003960. <https://doi.org/10.1371/journal.ppat.1003960>.
 27. van Gent M, Griffin BD, Berkhoff EG, van Leeuwen D, Boer IGJ, Buisson M, Hartgers FC, Burmeister WP, Wiertz EJ, Rensing ME. 2011. EBV lytic-phase protein BGLF5 contributes to TLR9 downregulation during productive infection. *J Immunol* 186:1694–1702. <https://doi.org/10.4049/jimmunol.0903120>.
 28. Bentz GL, Liu R, Hahn AM, Shackelford J, Pagano JS. 2010. Epstein-Barr virus BRLF1 inhibits transcription of IRF3 and IRF7 and suppresses induction of interferon- β . *Virology* 402:121–128. <https://doi.org/10.1016/j.virol.2010.03.014>.
 29. Hahn AM, Huye LE, Ning S, Webster-Cyriaque J, Pagano JS. 2005. Interferon regulatory factor 7 is negatively regulated by the Epstein-Barr virus immediate-early gene, BZLF-1. *J Virol* 79:10040–10052. <https://doi.org/10.1128/JVI.79.15.10040-10052.2005>.
 30. Wang JT, Doong SL, Teng SC, Lee CP, Tsai CH, Chen MR. 2009. Epstein-Barr virus BGLF4 kinase suppresses the interferon regulatory factor 3 signaling pathway. *J Virol* 83:1856–1869. <https://doi.org/10.1128/JVI.01099-08>.
 31. Wu L, Fossum E, Joo CH, Inn K-S, Shin YC, Johannsen E, Hutt-Fletcher LM, Hass J, Jung JU. 2009. Epstein-Barr virus LF2: an antagonist to type I interferon. *J Virol* 83:1140–1146. <https://doi.org/10.1128/JVI.00602-08>.
 32. Croft NP, Shannon-Lowe C, Bell AI, Horst D, Kremmer E, Rensing ME, Wiertz EJHJ, Middeldorp JM, Rowe M, Rickinson AB, Hislop AD. 2009. Stage-specific inhibition of MHC class I presentation by the Epstein-Barr virus BNLF2a protein during virus lytic cycle. *PLoS Pathog* 5:e1000490. <https://doi.org/10.1371/journal.ppat.1000490>.
 33. Horst D, van Leeuwen D, Croft NP, Garstka MA, Hislop AD, Kremmer E, Rickinson AB, Wiertz EJHJ, Rensing ME. 2009. Specific targeting of the EBV lytic phase protein BNLF2a to the transporter associated with antigen processing results in impairment of HLA class I-restricted antigen presentation. *J Immunol* 182:2313–2324. <https://doi.org/10.4049/jimmunol.0803218>.
 34. Quinn LL, Zuo J, Abbott RJM, Shannon-Lowe C, Tierney RJ, Hislop AD, Rowe M. 2014. Cooperation between Epstein-Barr virus immune evasion proteins spreads protection from CD8⁺ T cell recognition across all three phases of the lytic cycle. *PLoS Pathog* 10:e1004322. <https://doi.org/10.1371/journal.ppat.1004322>.
 35. Hislop AD, Rensing ME, van Leeuwen D, Pudney VA, Horst D, Koppers-Lalic D, Croft NP, Neeffes JJ, Rickinson AB, Wiertz EJHJ. 2007. A CD8⁺ T cell immune evasion protein specific to Epstein-Barr virus and its close relatives in Old World primates. *J Exp Med* 204:1863–1873. <https://doi.org/10.1084/jem.20070256>.
 36. Griffin BD, Gram AM, Mulder A, Van Leeuwen D, Claas FHJ, Wang F, Rensing ME, Wiertz E. 2013. EBV BILF1 evolved to downregulate cell surface display of a wide range of HLA class I molecules through their cytoplasmic tail. *J Immunol* 190:1672–1684. <https://doi.org/10.4049/jimmunol.1102462>.
 37. Zuo J, Currin A, Griffin BD, Shannon-Lowe C, Thomas WA, Rensing ME, Wiertz EJHJ, Rowe M. 2009. The Epstein-Barr virus G-protein-coupled receptor contributes to immune evasion by targeting MHC class I molecules for degradation. *PLoS Pathog* 5:e1000255. <https://doi.org/10.1371/journal.ppat.1000255>.
 38. Rensing ME, van Leeuwen D, Verreck FAW, Keating S, Gomez R, Franken

- KLMC, Ottenhoff THM, Spriggs M, Schumacher TN, Hutt-Fletcher LM, Rowe M, Wiertz EJHJ. 2005. Epstein-Barr virus gp42 is posttranslationally modified to produce soluble gp42 that mediates HLA class II immune evasion. *J Virol* 79:841–852. <https://doi.org/10.1128/JVI.79.2.841-852.2005>.
39. Rensing ME, van Leeuwen D, Verreck FAW, Gomez R, Heemskerk B, Toebes M, Mullen MM, Jardetzky TS, Longnecker R, Schilham MW, Ottenhoff THM, Neeffjes J, Schumacher TN, Hutt-Fletcher LM, Wiertz EJHJ. 2003. Interference with T cell receptor-HLA-DR interactions by Epstein-Barr virus gp42 results in reduced T helper cell recognition. *Proc Natl Acad Sci U S A* 100:11583–11588. <https://doi.org/10.1073/pnas.2034960100>.
40. Gram AM, Oosenbrug T, Lindenbergh MFS, Büll C, Comvalius A, Dickson KJ, Wiegant J, Vrolijk H, Lebbink RJ, Wolterbeek R, Adema GJ, Griffioen M, Heemskerk MHM, Tschärke DC, Hutt-Fletcher LM, Wiertz EJHJ, Hoeben RC, Rensing ME. 2016. The Epstein-Barr virus glycoprotein gp150 forms an immune-evasive glycan shield at the surface of infected cells. *PLoS Pathog* 12:e1005550. <https://doi.org/10.1371/journal.ppat.1005550>.
41. Cohen JI, Lekstrom K. 1999. Epstein-Barr virus BART1 protein is dispensable for B-cell transformation and inhibits alpha interferon secretion from mononuclear cells. *J Virol* 73:7627–7632.
42. Strockbine LD, Cohen JI, Farrah T, Lyman SD, Wagene F, DuBose RF, Armitage RJ, Spriggs MK. 1998. The Epstein-Barr virus BART1 gene encodes a novel, soluble colony-stimulating factor-1 receptor. *J Virol* 72:4015–4021.
43. Salek-Ardakani S, Arrand JR, Mackett M. 2002. Epstein-Barr virus encoded interleukin-10 inhibits HLA-class I, ICAM-1, and B7 expression on human monocytes: implications for immune evasion by EBV. *Virology* 304:342–351.
44. Levitskaya J, Coram M, Levitsky V, Imreh S, Steigerwald-Mullen PM, Klein G, Kurilla MG, Masucci MG. 1995. Inhibition of antigen processing by the internal repeat region of the Epstein-Barr virus nuclear antigen-1. *Nature* 375:685–688. <https://doi.org/10.1038/375685a0>.
45. Yin Y, Manoury B, Fähraeus R. 2003. Self-inhibition of synthesis and antigen presentation by Epstein-Barr virus-encoded EBNA1. *Science* 301:1371–1374. <https://doi.org/10.1126/science.1088902>.
46. Taylor GS, Long HM, Brooks JM, Rickinson AB, Hislop AD. 2015. The immunology of Epstein-Barr virus-induced disease. *Annu Rev Immunol* 33:787–821. <https://doi.org/10.1146/annurev-immunol-032414-112326>.
47. Li J, Callegari S, Masucci MG. 2017. The Epstein-Barr virus miR-BHRF1-1 targets RNF4 during productive infection to promote the accumulation of SUMO conjugates and the release of infectious virus. *PLoS Pathog* 13:e1006338. <https://doi.org/10.1371/journal.ppat.1006338>.
48. Feederle R, Haar J, Bernhardt K, Linnstaedt SD, Bannert H, Lips H, Cullen BR, Delecluse H-J. 2011. The members of an Epstein-Barr virus microRNA cluster cooperate to transform B lymphocytes. *J Virol* 85:9801–9810. <https://doi.org/10.1128/JVI.05100-11>.
49. Bernhardt K, Haar J, Tsai MH, Poirey R, Feederle R, Delecluse HJ. 2016. A viral microRNA cluster regulates the expression of PTEN, p27 and of a bcl-2 homolog. *PLoS Pathog* 12:e1005405. <https://doi.org/10.1371/journal.ppat.1005405>.
50. Poling BC, Price AM, Luftig MA, Cullen BR. 2017. The Epstein-Barr virus miR-BHRF1 microRNAs regulate viral gene expression in cis. *Virology* 512:113–123. <https://doi.org/10.1016/j.virol.2017.09.015>.
51. Delecluse HJ, Hilsendegen T, Pich D, Zeidler R, Hammerschmidt W. 1998. Propagation and recovery of intact, infectious Epstein-Barr virus from prokaryotic to human cells. *Proc Natl Acad Sci U S A* 95:8245–8250.
52. Murer A, McHugh D, Caduff N, Kalchschmidt J, Barros M, Zbinden A, Capaul R, Niedobitek G, Allday M, Chijioke O, Münz C. 2018. EBV persistence without its EBNA3A and 3C oncogenes in vivo. *PLoS Pathog* 14:e1007039. <https://doi.org/10.1371/journal.ppat.1007039>.
53. Berger C, Day P, Meier G, Zingg W, Bossart W, Nadal D. 2001. Dynamics of Epstein-Barr virus DNA levels in serum during EBV-associated disease. *J Med Virol* 64:505–512.
54. Bickham K, Goodman K, Paludan C, Nikiforow S, Tsang ML, Steinman RM, Münz C. 2003. Dendritic cells initiate immune control of Epstein-Barr virus transformation of B lymphocytes in vitro. *J Exp Med* 198:1653–1663. <https://doi.org/10.1084/jem.20030646>.